A MODEL FOR SPIKE GENERATION IN PRIMARY AUDITORY NEURON

Yasuhumi Ono

Torao Yanaru

Yasuyuki Iso

SUMMARY

A new model which is based on the following four assumptions is proposed. 1. There are spontaneous releases of packets of chemical transmitter from the hair cell. The releases follow Poisson's law. 2. The average rate of the releases is propotional to the exponential function of depolarization potential of the hair cell menbrane. 3. The depolarization is propotional to the cochlear microphonics. 4. Chemical transmitter causes the post synaptic potential (PSP) in the nerve endings, and when the PSP reaches a threshold value, a spike is generated.

The response of the model to sinusoidal inputs is investigated. Phase-locked histograms and pulse interval histograms are obtained, and are compared with those of biological neurons. Considerable discrepancy is observed between the pulse interval histograms of the model and those of biological neurons. A probable explanation of this discrepancy is suggested.

INTRODUCTION

The aims of this study are two-fold ; the one is to provide an example of density modulated random pulse trains, the other is to present a working hypothesis about a possible mechanism of spike generation in primary auditory neurons. Although the mechanism of spike generation (in primary auditory neurons) has not yet been known, there are at least two lines of clues which suggest the mechanism, the fist is the spike pattens from single fibers of auditory nerves, and the second is the structure of hair cells (recepter cells).

In recent years, a considerable amount of data concerning the discharge pattern of single fibers of auditory nerves under various stimulus conditions has become availa-ble.[1],[2][3] It is found out that many fibers exibit spontaneous discharges. According to Kiang et al., time pattens of the spontaneous activity have the following properties.

(i) All units examined by them displayed some spontaneous activity. (ii) The average rates for different units varied from less than 6 spikes/min to approximately 100 spikes/sec. (iii) The shapes of interspike interval histograms rise quickly to a peak, usually before 10 msec, regardless of the rates of discharge, and then decay exponentially. (iv) Successive intervals are nearly independent.

Thus, the spike trains of spontaneous discharges are very close to homogeneous Poisson pulse train, except that, the number of short intervals is much smaller in the

pulse trains of spontaneous discharge than in the Poisson pulse train. This difference is assumed to be the consequence of refractory property of the units. The response of primary auditory nerves to low frequency tones[1] also shows time patterns which are very similar to that of Poisson pulse trains modulated by the tones. The similarity holds well for wide range of frequencies and intensity of the tones.

These facts suggest the process of random pulse generation and modulation, underlying the spike generation mechanism. Recent electron micrographic studies have revealed that the structure of the junction between the hair cell and nerve endings is very similar to the structure of chemical synapses.

It will be quite promising to investigate the model which is composed of random pulse modulator and a model of synaptic transmission.

As the case corresponding to the spontaneous discharges of the model was reported previously,[4] the response to sinusoidal inputs is investigated below. This report consists of three sections. Section 1 describes the structure of the model. Section 2 deals with the measurement of two kinds of histograms. In section 3 the results of the measurement are shown and briefly discussecd.

1. Model

The model is based on the following basic assumptions.

A. 1. Packets of chemical transmitter are released spontaneously from the hair cell. The releases follow Poisson's law.

A. 2. The average rate of the releases is proportional to the exponential function of the hair cell depolarization potential.

A. 3. The depolarization potential is proportional to the cochlear microphonics.

A. 4. The transmitter produces the post synaptic potential (PSP) in the nerve endings, and when the PSP reaches a threshold value, a spike is generated. The phenomenon of A. 1, i.e., the spontaneous release of transmitter and its Poisson nature has been firmly established at neuro-muscular synapses, and has been known as miniature endplate potentials (min. EPPs). The same is assumed to be true for most chemical synapses. A. 2. also agrees with the observed relationship about the min. EPPs. But as the data about the detailed time course of average rate in response to a given change in nerve ending depolarization is not yet available, the average rate is assumed to follow exactly to the time course of the exponential function of menbrane potential. The cochlear microphonic is believed to be generated at the boundary between hair cell and scala media. It will be quite natural to assume as in A. 3 that the potential of hair cell menbrane also varies propotionally with the cochlear microphonic. The question which of the two is the cause of the other has no relevance here. A. 4 is the basic process which is commonly observed at all chemical synapses. Fig 1. 1 shows the circuit diagram of the model. The whole circuit is composed of two parts : a hair cell model and a neuron model.

The hair cell model is essentially a random pulse generator, which can be density modulated in accordance with the exponential function of input voltage. It is found[4] that the randon pulse generator using a zener diode under suitable bias current is almost ideal for this purpose, i.e., it generates Poisson pulses, the logarithm of the average rate is linearly related to the bias
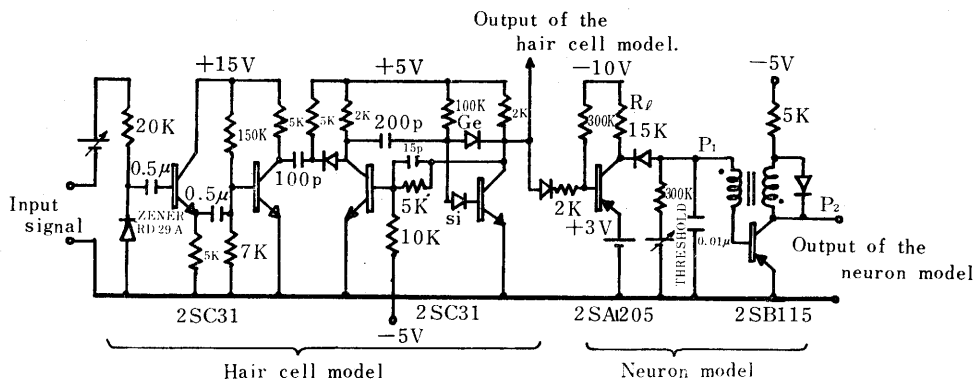
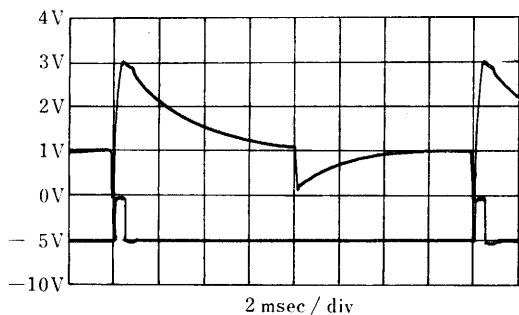Fig. 1.1 The circuit diagram of the model

2 msec / div

Fig. 1.2 Voltage wave form on the point P_1
and P_2 in Fig 1.1

upper trace : P_1

lower trace : P_2

current over considerable range of rate.

Thus it satisfies the conditions A. 1 and A. 2. The remainder part of the hair cell model is the shaper of pulses to the standard rectangular shape of -10 volts height and 20 μsec duration. The neuron model is a blocking oscillator composed of an RC filter and threshold element, as is clear from the figure. The time constant of the RC filter corresponds to that of PSP decay and is set at about 3 msec. The threshold value can be adjusted by the bias voltage, and the
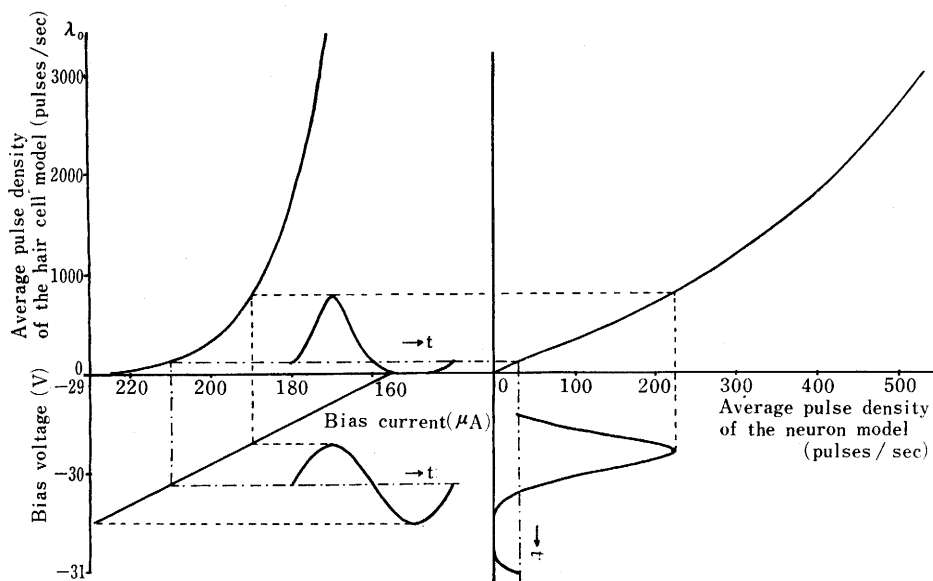

Fig. 1.3 Static characteristics of the model

magnitude of unit PSP is adjustable by the Resistance R_t. In this study, the threshold is chosen very low, at about 1.1 times of the magnitude of unit PSP, because of the reason described later. The base voltage has some overshoot after a pulse, like the after-hyperpolarization in biological neuron. Fig 1.2 shows the voltage wave form on the point P_1 and P_2 in Fig 1. 1.

The static characteristics of the model are shown in Fig 1.3. The relation of the bias voltage and current of the noise diode is drawn on the left lower part of the figure.

The left upper part shows the average pulse density λ_0 of the hair cell model as a function of the bias current. The relation is very nearly exponential in the shown range of average density. Moreover the Poisson nature of the pulse trains is confirmed in the same range. In the right upper part is shown the static characteristic of the neuron model, the ordinate is the input pulse density and the abscissa is the output pulse density. In the figure is also shown changes in pulse densities of the output of the hair cell model and neuron model, when the sinusoidal voltage of very low frequency is applied to the input of the hair cell model. The curves correspond to the case, when a sinusoidal voltage of 0.8 volts peak to peak is superposed to DC bias voltage of 30.1 volts. These curves are used later for comparison with the results of measurements. The measurements are carried out for various combinations of the following values of three kinds of paramaters

(i) average density; $\lambda_0 = 0$, 120, 750 pulses 1 sec.

(ii) sinusoidal peak to peak voltage; 0.2V, 0.4V, 0.6V, 0.8V, 1.0V, 1.3V.

(iii) frequency of sinusoidal voltage; 200Hz, 400Hz, 620Hz, 780Hz, 980Hz, 1880Hz.

2 Methods of measurements

It is desirable that the data about all the pulse intervals of a sample pulse train are collected, and then processed by the digital computer. But, as the reliable recorder and other necessary instruments are not available, the following methods are attempted.

2.1 Measurement of phase-locked histograms
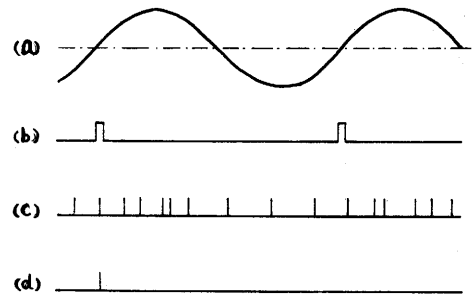
Fig. 2.1 shows the principle of measurement.

Fig. 2.1 The principle of measurement of phase-locked histogram

(a) is the input sinusoidal voltage, (b) shows the gate pulses which are synchronized to the input signals and have a constant duration; 1/16 of one period.

(c) is the random pulses and (d) is the pulses which have passed through the gate. If the pulses (d) are counted for several seconds, the number for one bar of the histogram is obtained. The gate pulses are switched to the next position and the same procedures are repeated until the whole period is covered, then the histogram is completed.

As shown in Fig. 2.2, the gate pulses are made by appropriately combining through the "and" gate the four square waves, which have the frequencies of 1 2, 4 and 8 times respectively, as high as the fre-
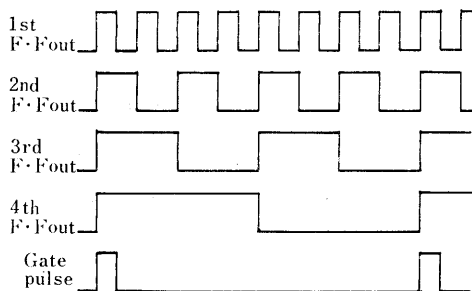
Fig. 2.2 Method of gate pulse generation

Fig. 2.3 Block diagram of gate pulse generator
(shows a flip-flop)

quency of the modulating signal. In the figure is shown the first position. Thus, any one of the sixteen positions can be selected by switches. Actually the successive selection is made automatically by electronic iswtches. Fig. 2.3 shows the arrangement
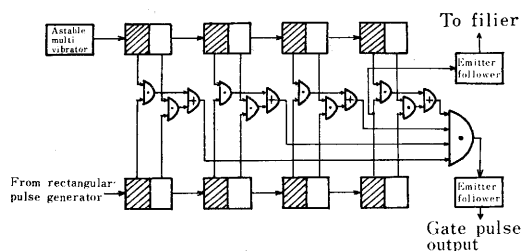
of this procedure. The lower sequence of flip-flops is the gate pulse generator, and the upper row generates the control signal for the selection of switch. The block diagram of the whole circuit for the measurement is given in Fig. 2.4. The counted
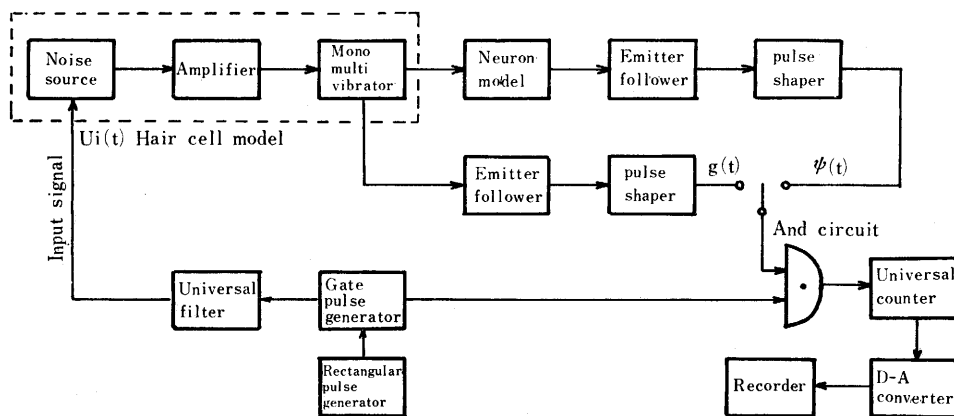

Fig. 2.4 Block diagram of whole circuit for the measurement of phase-locked histogram

numbers are converted to analog quantities by a D-A converter, and recorded as a complete phase-locked histogram by the recording instrument.

2.2 Measurement of pulse interval histograms

The gate pulses described in 2.1 can also be used to get pulse interval histograms. Let us suppose that an interval histogram is devided into 16 groups according as positions of start pulses, i. e., if a start pulse

of an interval falls in the ith gate position, the interval belongs to the ith group. The number of intervals in the ith group must be proportional to $R(t_i) \cdot \Delta$, where t_i is the representative instant of the ith gate position, $R(t_i)$ is the instantaneous pulse density of the given pulse train, and Δ is the width of the gate. When all the groups are added together, they naturally result in the original histogram. Assume that the counter is reset at constant rate, called

158

reset cycle, the period of the reset cycle is T_r, an instant of a reset pulse is denoted by t_1, and t_2 is the first upward zero crossing of the input signal after t_1. If a pulse of the random pulse train falls in the first gate after t_2, the interval from that pulse to the next is counted and recorded, otherwise the all pulses in that reset cycle are abandoned.

If the interval measurements are carried out for long enough time T, one group of histogram corresponding to the gate position is obtained. When the same procedure is repeated as many times as the number of gate positions, and all the groups of histograms are added together, the result is the required pulse interval histogram.

3 Results

For the sake of convenience of description, the following symbols will be used bellow.

$v_i(t)$; input signal.

$g(t)$; output pulse train of the hair cell model, or input pulse train to the neuron model.

$\psi(t)$; output pulse train of the neuron model.

$\lambda(t)$; instaneous pulse density of $g(t)$.

λ_0 ; average value of $\lambda(t)$.

λ_n ; pulse density of $g(t)$, when input A-C voltage is zero.

S ; synchronization coefficient, S is defined by Rose et al., as the percentage of number of pulses which occur during the most effective half of the modulating cycle.

N ; total number of pulses in a histogram.

3.1 Phase-locked histograms

Fig. 3.1 shows the phase-locked histograms of $g(t)$ and $\psi(t)$ in the left and right rows respectively. The frequency of input signal $v_i(t)$ is 200 Hz. Pulses are counted during 10 seconds for each gate position.
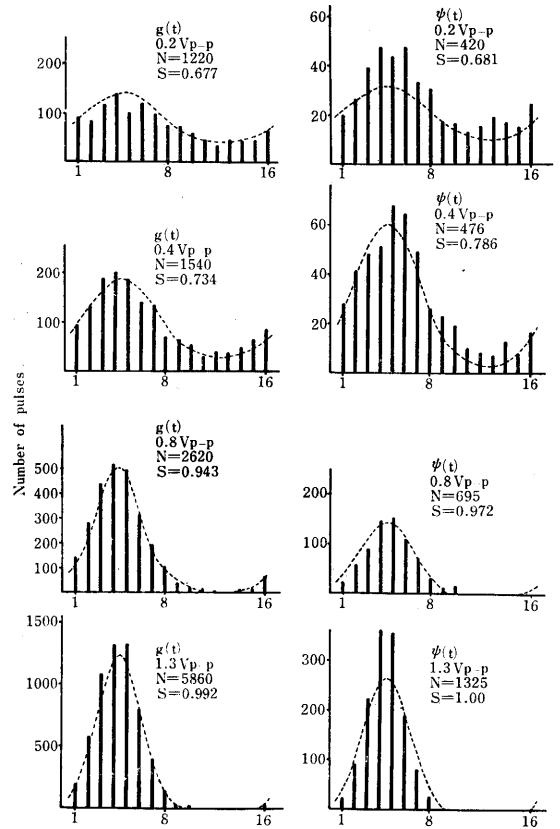

Fig. 3.1 Phase-locked histograms of g(t) and $\psi(t)$. The frequency of $v_i(t)$=200Hz, λ_n = 120

The histograms are taken three times under the same conditions for each cace, but only one for each is shown. Dotted curves in the figure are waveforms of $\lambda(t)$ obtained from the static characteristic (simply called static waveforms) by the method illustrated in Fig. 1.2. From the figure, we can see that the histograms of $g(t)$ agree very well with the corresponding static waveforms, and those of $\psi(t)$ also agree fairly well each other. Fig. 3.2 shows the total number N in a histogram, and synchronization coefficient S against input voltage. For each input voltage, three points are plotted, corresponding to the above mentioned three histograms. Values of N and S calculated from static waveforms are also drawn in
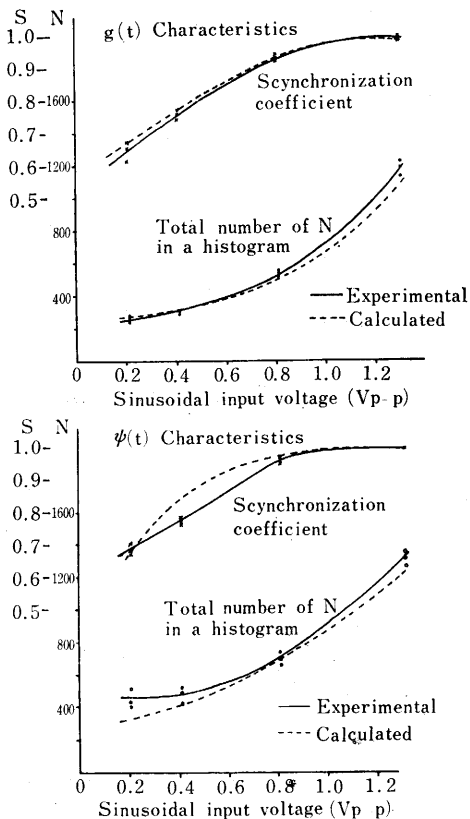
Fig. 3.2 **The number of pulses in a histogram**
and Scynchronization coefficient.
The frequency of v_i $(t) = 200$Hz, $\lambda_n = 120$

constant at 0.4 volts peak to peak. The similar results are shown in Fig. 3.4, when the input voltage is 1.3 volts peak to peak.

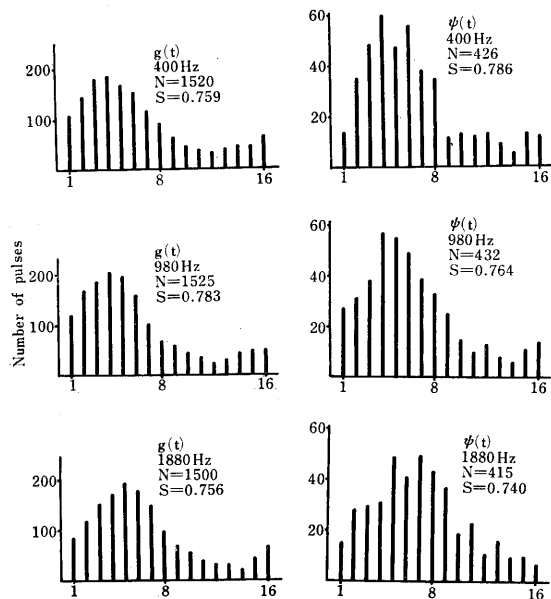Fig. 3.3 **Phase-locked histograms of** $g(t)$.
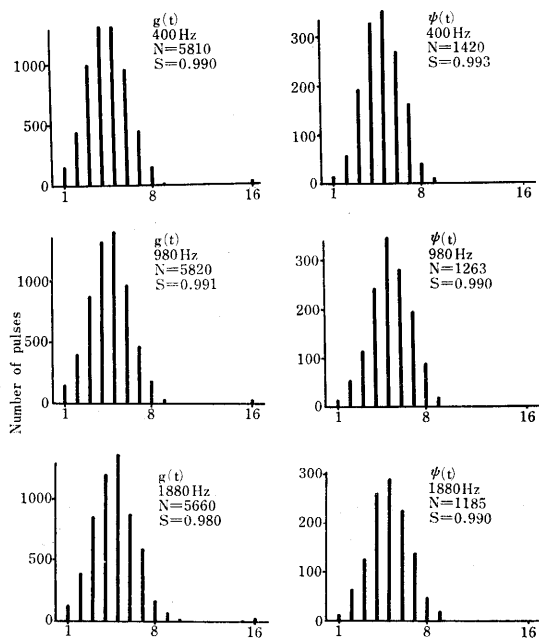**The input voltage is 0.4** V_{p-p}, $\lambda_n = 120$

the figure. Again, agreement between the results obtained from the histograms and those derived from the static wave forms is good for $g(t)$, but small differences are observed between the two kinds of results for $\psi(t)$. The reason for this differences is not clear. The histogram of $\psi(t)$ seems to have a small phase lag compared with the histogram of $g(t)$, or the input signal, when the input voltage is small. Next, let us examine the effect of input frequency on the shape of histograms. In Fig. 3.3, the histograms are shown for three different input frequencies, input voltage being held

Fig. 3.4 **Phase-locked histograms of** $g(t)$ **and** $\psi(t)$.
The input voltage is 1.3 V_{p-p}, $\lambda_n = 120$

We can see little differences among the shapes of histograms of $g(t)$ for the change in input frequencies. This means that the density modulation of random pulses is performed without time lag. But as for the histograms of $\psi(t)$, We can notice some differences in shape as the input frequencies are changed, i. e., the peak of the histograms become smaller as the frequency is made higher. This fact is also reflected in the S value.

In Fig. 3.5 and 3.6, the histograms of $\psi(t)$ for different input frequencies are shown, when λ_n is chosen to be zero and 750 respectively. When $\lambda_n = 0$, i.e., when the model works at low pulse density region, the same trend as described in relation to Fig. 3.3 is observed, but when $\lambda_n = 750$, the trend is not obvious.
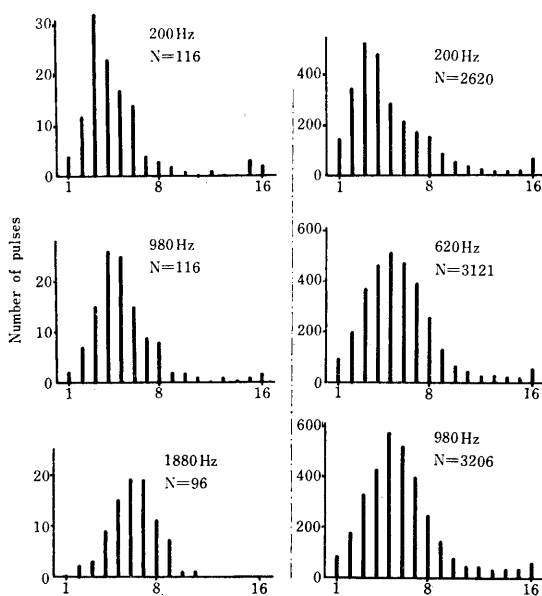

Fig. 3.5 Phase - locked histograms of $\psi(t)$. The input voltage is 1 V_{p-p}, $\lambda_p = 0$

Fig. 3.6 Phase - locked histograms of $\psi(t)$. The input voltage is 0.8 v_{p-p}, $\lambda_n = 750$

3.2 Pulse interval histograms

Fig. 3.7, 3.8, 3.9, show the pulse inter-val histograms for the input frequencies of 200Hz, 600Hz, and 980Hz respectively.

The histograms of $g(t)$ are shown in the left rows and those of $\psi(t)$ are shown in the right rows. The histograms of $g(t)$ seem to have general shape which can be expressed as the product of an exporential function and a periodic function with the period of the input signal. Thus they are very similar to the histograms of periodically modulated Poisson pulses.[5] These pulse interval histograms also indicate the Poisson nature of the output pulse trains of the hair cell model. the histograms of $\psi(t)$ are also poly-modal, and distances between successive peaks of the modes are nearly equal to the period of input signal. But there is one difference between the histograms of $\psi(t)$ and those of $g(t)$, i.e., in the former, short intervals are lacking. Consequently the peak of each mode is proportional not to an exporential curve, but to a gamma distribution curve. We shall discuss this point further in the next paragraph.

DISCUSSION

When we compare these results with those of Rose et al., we may say that the main features of the phase-locked histograms of the both results are in good agreement with each other. But as for the pulse interval histograms, there is one definite difference between these two cases. The number of short intervals is much smaller in the histograms of the model, than in those of biological neurons.

The histograms of biological neurons are more like our histograms of $g(t)$ than those of $\psi(t)$. We shall focus our attention chiefly to this difference. If more close resemblance is wanted without changing the basic assumptions of the model, there are
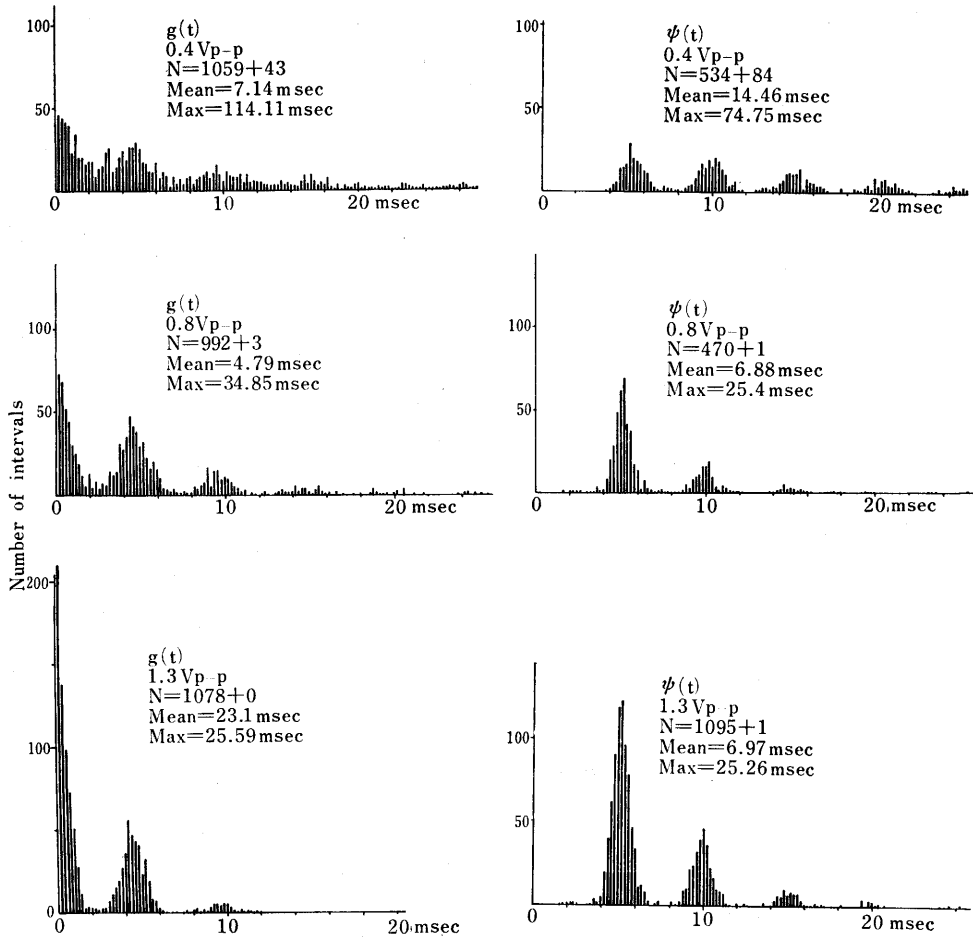
Fig. 3.7 Pulse interval histograms of g(t) and ψ(t).

The frequuency of ν_i (t) = 200Hz, λ_n = 120

two possibilities to be examined. The one is to assume that the neuron model has the threshold value which is smaller than the magnitude of unit PSP, and has very short refractory period. The other is to assume that each auditory nerve innervates several hair cells, so that the observed spike train is actually the result of supperposition of several spike trains from those hair cells.

In the first assumption, there are some difficulties. The largest of all is concerned with the response pattern of primary auditory neurons to click stimuli. [3]

Although we do not have enough space to discuss this problem, it seems to be reasonable to consider that the magnitude of unit PSP is much smaller than the threshold. As a matter of fact, in this study, we chose the very low threshold value, which is 1.1 times the magnitude of unit PSP, to examine how the histograms of $\psi(t)$ come close to the histograms of $g(t)$. The difference between these two kinds of histograms is largely attributable to the overshoot of the neuron model after the pulse generation, or the
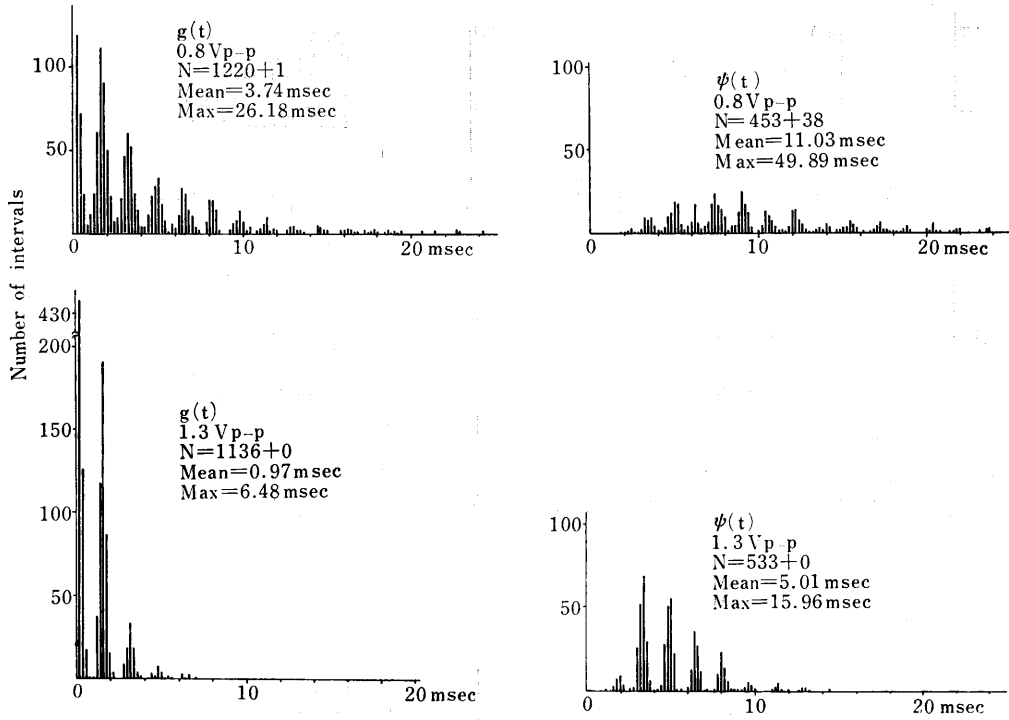
162

Fig. 3.8   Pulse interval histograms of g(t) and ψ(t).
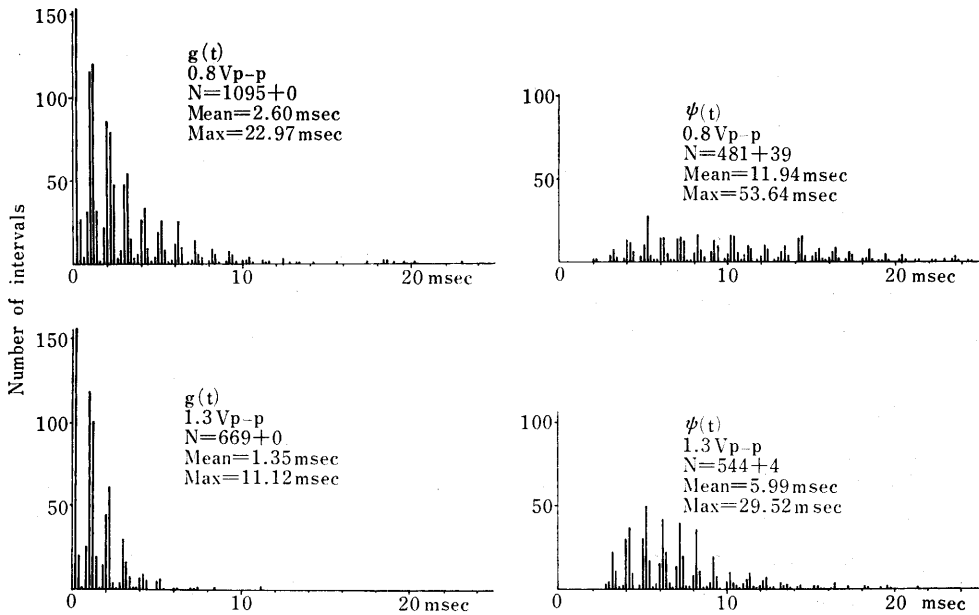
The frequency of v_i (t)=620Hz, λ_n =120

Fig. 3.9   Pulse interval histograms of g(t) and ψ(t)   The frequency of v_i (t)=980Hz, λ_n =120

N·B. N is given as the sum of two numbers.   The first indicates the number of plotted intervals, the second is the number of intervals whose values exceed the maxmal value of the abscissa.

refractory property of the model. If the overshoot is made smaller, the difference would be smaller.

But from several reasons, the second assumption seems to be more probable, it seems to be able to account for several features of spike trains. The shape of pulse interval histograms and the response pattern to clicks are two examples. Characteristic shape of hazard function of pulse intervals studied by Gray[6] also supports this assumption. We are now making investigation along this line.

References

1. J.E. Rose, J.F. Brugge, D.J. Anderson, and J.E. Hind. Phase-locked response to low-frequency tones in single auditory nerve fivers of the squirral monkey. J.Neurophysiol. **30**; 769~793, 1967.

2. M.Nomoto, N.Suga, and Y.Katsuki. Discharge pattern and inhibition of primary auditory nerve fibers in the monkey. J.Neurophysiol. **27**; 768~787, 1964.

3. N.Y. Kiang. Discharge patterns of single fibers in the cat's auditory nerve. M.I.T. Reserch Monograph No. 35. The M.I.T. press.

4. Y.Nakayama, T.Yanaru and Y.Iso. A simple noise generator by a microplasma. Bulletin of the Kyushu Institute of Technology. 1968.

5. Y.Iso. Density modulation of random pulse train. Bulletin of the Kyushu Institute of Technology. 1969.

6. P.R. Gray. A statistical Analysis of electrophysiological data from auditory nerve fivers in cat. M.I.T. Technical report **451**. June, 1966.